ORIGINAL RESEARCH (AR) DOI: 10.4274/jems.2024.46693

Journal of ETA Maritime Science 2024;12(3):277-286

Blade Stress of Carbon Fiber B-Series Marine Propellers Based on Numerical Analysis

Firly Irhamni Ahsan, I Made Ariana, Aguk Zuhdi Muhammad Fathallah

Institut Teknologi Sepuluh Nopember, Department of Marine Engineering, Surabaya, Indonesia

Abstract

In the maritime world, carbon composite material has been used as a propeller on ships. Research on the use of carbon composite materials began in the early 2000s. With features including reduced cavitation and pressure fluctuations, improved acoustic attenuation, corrosion resistance, lower maintenance costs, enhanced efficiency, and longer propulsion system service life, carbon composite materials offer several benefits. The propeller's strength and performance should increase with the use of carbon composite materials. This research uses the Fluid Structure Interaction method by conducting computational fluid dynamic simulations followed by finite element analysis. This study analyzed the deformation and stress on the propeller blades by comparing epoxy carbon fiber that was woven and unidirectional with quasi-isotropic laminate; additionally, it will be compared with other metal materials like bronze, titanium alloy, and copper alloy. Through the process of study and observation of the numerically derived data, which represent the propeller blade's maximum deformation and equivalent stress. By comparing two types of carbon fiber, it can be analyzed from the results of maximum deformation and equivalent (Von-Mises) stress using the fluid structure interaction method. The results show that the epoxy carbon fiber is five times lighter than the copper alloy material, and the stress distribution has a similar pattern, but the deformation results of the two epoxy carbon fiber materials differ from those of the metal materials.

Keywords: Marine-propeller, CFRP propeller, Carbon fiber, Open water test, Fluid-structure interaction

1. Introduction

Composite propellers are more technologically advanced than traditional metal propellers because they have better acoustic attenuation, less cavitation and pressure fluctuations, less magnetic interference, lower maintenance costs, and longer propulsion system service lives. Examples of these composite propellers are those made of manganese-nickel-aluminum bronze and nickel-aluminum bronze [1-3]. Aside from all of these advantages, a particular alignment of the fibers can improve the propeller's flexibility and weight-carrying capacity. This prevents flapping by enabling the propeller to autonomously modify its form based on flow conditions and rotational speed [4]. A computational fluid dynamics (CFDs) approach was used for a number of propeller analyses, such as determining how a pre-duct affects ships with Propeller-Hull Interactions, altering the trailing edge shape to make it less likely to singe, assessing the propeller's performance, and using numerical methods to find cavitation noise in marine skew propellers [5-7].

The propeller's complex shape and loading conditions make structural analysis challenging. The propeller's structure can be studied using two main methods: analytical techniques and numerical analysis. The theories of curved beams, plates, and shells, and Taylor's approach, are examples of analytical techniques [8]. The numerical method computes the displacement and stresses quantitatively using finite element method (FEM) solvers [9]. Researchers at Bureau Veritas, a classification society, have recently developed an analytical method tailored to composite propellers. Based on the cantilever beam method, this method produces findings that are quite similar to numerical ones [10]. Compared with numerical methods, the ten analytical methods are faster, simpler, and easier to use. However, because of the assumptions made to simplify the problem, the solutions

Address for Correspondence: Firly Irhamni Ahsan, Institut Teknologi Sepuluh Nopember, Department of Marine Engineering, Surabaya, Indonesia
E-mail: firlyiahsan@gmail.com
ORCID iD: orcid.org/0000-0001-7843-6320

Received: 04.01.2024
Last Revision Received: 25.04.2024
Accepted: 05.06.2024

To cite this article: F. I. Ahsan, I. M. Ariana, and A. Z. M. Fathallah, "Blade Stress of Carbon Fiber B-Series Marine Propellers Based on Numerical Analysis." *Journal of ETA Maritime Science*, vol. 12(3), pp. 277-286, 2024.

are less precise. On the other hand, numerical procedures produce greater precision but require more time and money to process computationally.

Using the commercial program ANSYS Workbench, we investigated the hydrodynamic and structural characteristics of a large screw, seven-bladed composite propeller. Their findings demonstrated that it is critical to consider the effects of FSI when analyzing flexible composite propellers [11]. Using numerical modeling in one-way coupled situations, it is possible to forecast the fatigue life of the two naval propellers. In addition, they used coupled FSI assessments for various currently used materials, including stainless steel and aluminum alloy [12]. The bidirectional FSIs of glass fiber composite propellers and nickel-aluminum bronze propellers is calculated using finite element software and CFDs based on viscous flow theory [13]. Numerous studies that evaluated copper and composite propellers discovered that the latter are more vulnerable to hydrodynamic loads [14-16].

Propeller blades can be made of a composite material consisting of fibers and resin to lessen the cavitation impact (up to 70 percent) [17]. Composite materials can decrease cavitation damage while simultaneously enhancing fatigue resistance, corrosion resistance, and damping performance [18]. After several studies on the potential of carbon fiber in marine propellers, many more potentials need to be investigated. One such potential is the use of carbon fiber in patrol boats or fast boats, for which the stress on the material when it meets the pressure generated by the rotating propeller needs to be examined. As a result, CFDs and lifting surface theory can be used to assess thrust performance. Metallic materials such as bronze, titanium alloy, and copper alloy will be used for comparison.

2. Methodology

2.1. Geometrical Propeller B-5 Series

This study used the Wageningen B-5 Series propeller. An illustration of the propeller geometry can be seen in Figure 1.

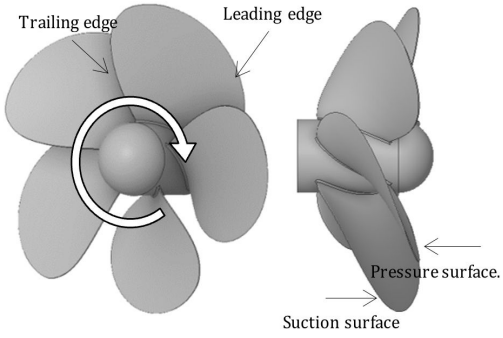

Figure 1. *Geometry of the propeller B-5 series*

Data can be found in Table 1, and it will be used as a research object for analyzing their effect using CFD simulation using the Open Water Test method from J=0 until J=1. By using this method, the pressure distribution will be produced on the propeller blade. In this study, only one blade representing the propeller will be analyzed. The blade model on the propeller is in Figure 2.

Table 1. *Geometrical parameters of the propeller B-5 series*

Parameter	Value
Diameter (mm)	290
AE/AO	1.05
P/D	1.1
Propeller Orientation	Right-hand Rotation
Number of Blades (Z)	5
Rotational Speed (RPM)	600

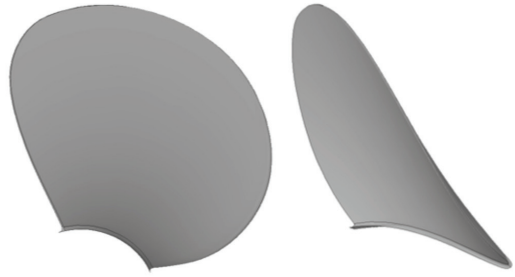

Figure 2. *Geometry of the blade propeller*

2.2. Propeller Theory

Hydrodynamic characteristics are a set of dimensionless coefficients that express a propeller's relative performance with respect to its mechanical attributes and fluid conditions. These parameters were designed to allow different propeller sizes and types to be compared. The propeller model was tested in open water to determine the intrinsic propeller performance while the ship was moving forward without the distribution of the ship. The terms thrust (T), torque (Q), and efficiency (η) are frequently used to describe the CFD results. With the torque coefficient (KQ) and thrust coefficient (KT) dimensionless and plotted against the advance ratio, the performance statistics are given in (J). The following non-dimensional terms are used to express the performance [19]:

$$K_t = \frac{T}{\rho n^2 D^4} \quad (1)$$

$$K_q = \frac{Q}{\rho n^2 D^5} \quad (2)$$

where n is the speed at which the propeller rotates, the propeller diameter is D, the fluid density is r, T is thrust, and

Q is torque. Furthermore, the advance ratio J, a dimensionless coefficient, is used to show the ratio of propeller speed Va to propeller tip speed:

$$J = \frac{V_a}{nD} \tag{3}$$

Finally, the propeller's open-water efficiency can be calculated as follows:

$$\eta = \frac{J}{2\pi}\frac{K_t}{K_q} \tag{4}$$

where ρ is the water density, n the number of propeller rotations per second (RPS)D is D the propeller diameter, and va represents water advance velocity (m/s).

2.3. Hydrodynamic Analysis

The flow around a marine propeller was effectively solved using Fluent, an unstructured mesh finite volume solution. The finite volume method applies Newton's second law in a model of fluid flow. The problem was resolved using the linear momentum conservation principle in the global Navier-Stokes equation. A few identities that are highly helpful for converting an equation of conservation for a quantity per unit mass to a quantity per unit volume can be derived using mass conservation.

Continuity equation:

$$\frac{\partial \rho A}{\partial t} + \nabla \cdot \rho A v = \rho \frac{DA}{Dt} \tag{5}$$

RANS equation:

$$\rho uj \frac{\partial ui}{\partial xj} = \rho fi + \partial\, \partial xj \left[-p\delta ij + \mu\left(\frac{\partial ui}{\partial xj} + \frac{\partial \mathrm{uj}}{\partial \mathrm{xi}}\right) - \rho u_i' u_j'\right] \tag{6}$$

The variables S, μui for liquid density, kg/mm^3, μ for turbulent viscosity, and p for static pressure, measured in Pa, are all related to the Reynolds stress term. The rotating coordinate system of the propeller is used in the computation, which is performed under stable conditions. The governing equations are the incompressible Newtonian fluid continuity equation and the Reynolds-averaged Navier-Stokes equations. Fluent version 2021 R2, a commercial CFD package, was used as the solver. The following equations express the k-ε Shear Stress Transfer (SST) turbulence model used in this study:

$$\rho \frac{Dk}{Dt} = \frac{\partial}{\partial x_i}\left[\left(\mu + \frac{\mu_t}{\sigma_k}\right)\frac{\partial k}{\partial x_i}\right] + G_k + G_b - \rho\varepsilon - Y_M \tag{7}$$

$$\rho \frac{D\varepsilon}{Dt} = \frac{\partial}{\partial x_i}\left[\left(\mu + \frac{\mu_t}{\sigma_k}\right)\frac{\partial \varepsilon}{\partial x_i}\right] + C_1\frac{\varepsilon}{k}(G_k + C_3 G_b) - C_2\rho\frac{\varepsilon^2}{k} \tag{8}$$

where k represents the energy of turbulent kinetics, reflects the rate of turbulent dissipation, is the amount of kinetic energy that is turbulent due to buoyancy, and is the energy released during turbulent turbulence when a fluid particle's average velocity gradient changes. While the constant coefficients are C_1, C_2, and C_3, YM denotes the influence of turbulent fluctuation expansion on the overall dissipation rate. The viscosity coefficient of the turbulence is represented by. Open-water numerical models were used to determine the propeller's hydrodynamic and hydroacoustic characteristics, which were later confirmed by the propeller's hydrodynamic performance [20]. The current computational approach for forecasting the hydrodynamic performance of cavitating and non-cavitating propellers in open water situations is accurate and reliable [21].

The hydrodynamics of propellers are computed numerically and contrasted with available experimental data. Then, the propeller's hydrodynamic force is applied using the finite element approach in open water, and the axial strain and corresponding force of propellers made of various materials are calculated along with their size and distribution. This information can serve as a theoretical foundation for propeller design optimization [22].

2.4. Boundary Conditions

CFDs modeling of open water tests serves as the boundary condition for this study. There are B-5 propellers, rotating domains, and static domains in these boundary conditions. And condition the position of the intake and outlet of the seawater. Compared with employing a reduced scale, the results are more accurate when the size of the modeling is made in accordance with the original or true scale, which brings the modeling closer to real conditions.

Three domains are identified in the initial development of this boundary condition: rotating domain, static domain, and propeller with hub. The static and rotating domains were originally joined to create space for the rotating domain. Because this domain is fluid, it is essentially used as a stream of water. Use vacuum or empty domains in static domains with hubs and rotating domains themselves to replicate open-water testing conditions found in real life. Figure 3 shows a comprehensive domain determination.

Velocity-inlet is the zone name that has been set on the meshing and previously in the inlet boundary conditions.

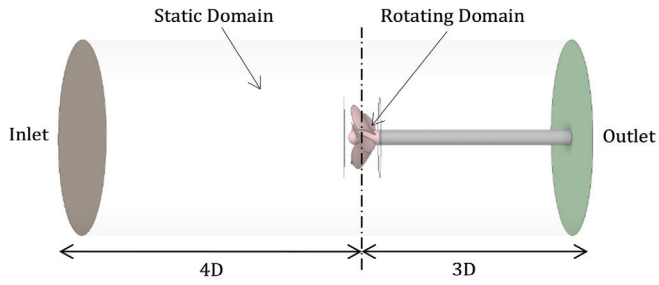

Figure 3. *Geometry of the computational domain of the B-5 propeller*

Therefore, it is filled in by inputting the flow velocity value in meters per second (m/s). In this case, the speed value is derived from the value of Va (advanced Velocity). Va can be a parameter that is entered as the initial Va at a speed of 0 m/s because this open-water test inputs variations in the value of Va based on the value of J.

Since this output is the consequence of the propeller's motion, the pressure at the outlet is set to 0, and the CFD solver computes the value. Considering that the propeller's diameter is four times the outlet's maximum seawater discharge. Fluent adapts to 1 atm conditions for operational conditions. The mesh configuration on the propeller and the domain is shown in Figure 4.

2.5. Fluid Structure Interaction

Therefore, loads and stresses must be computed simultaneously using hydrodynamic and structural analyses to precisely predict the performance of composite propellers. This relationship is called fluid-structure interaction analysis [23].

In the third section, the propeller hydrodynamics are estimated numerically. In contrast to the experimental evidence that has been published. The strength research and computation are then completed by applying the hydrodynamic force to the propeller using the FEM.

Utilizing the fluid-solid interaction analysis methodology, which combines a CFD approach based on the RANS equation with a FEM method for composite structures, the composite propeller's mechanical performance analysis is finished. Using the pressure-based solver and the k-w SST model, the CFD technique analyzes the propeller's hydrodynamic performance in all simulations. A fluid-solid interface is how the blade's surface is set up.

2.6. Materials Assignment

The material used in this study is epoxy carbon fiber, with two comparisons, namely unidirectional and woven fabric. First, epoxy (EP) matrix, high-strength carbon fiber unidirectional tape prepreg, quasi-isotropic laminate (0/+45/-45/90) s (unidirectional tape prepreg, fiber Vf: 0.55-0.65, autoclave cure at 115-180 °C, 7-6 bar) (Table 2).

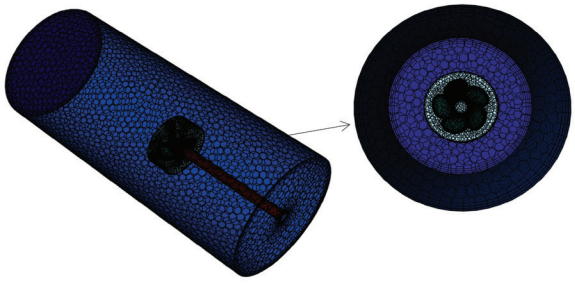

Figure 4. *Meshing configuration of the B-5 propeller*

Second material, epoxy (EP) matrix, high-strength carbon fiber woven fabric prepreg, quasi-isotropic laminate (0/90/+45/-45) s (woven fabric prepreg, fiber Vf: 0.48-0.58, autoclave cure at 120-180 °C, 6-7 bar). The material properties can be seen in Table 3, these two materials will also be compared with two other materials such as titanium alloy and copper alloy. The properties of the materials are shown in the table below. Therefore, in this analysis, 2 of the lightest carbon fiber materials were taken, namely epoxy carbon fiber UD and epoxy carbon fiber Woven with mass of 8.65E-02 kg and 8.71E-02 kg respectively. When compared to metallic materials such as copper alloys with non-metallic materials such as epoxy carbon fiber UD, obtained a ratio value of 1: 5. The material comparison is illustrated in Figure 5.

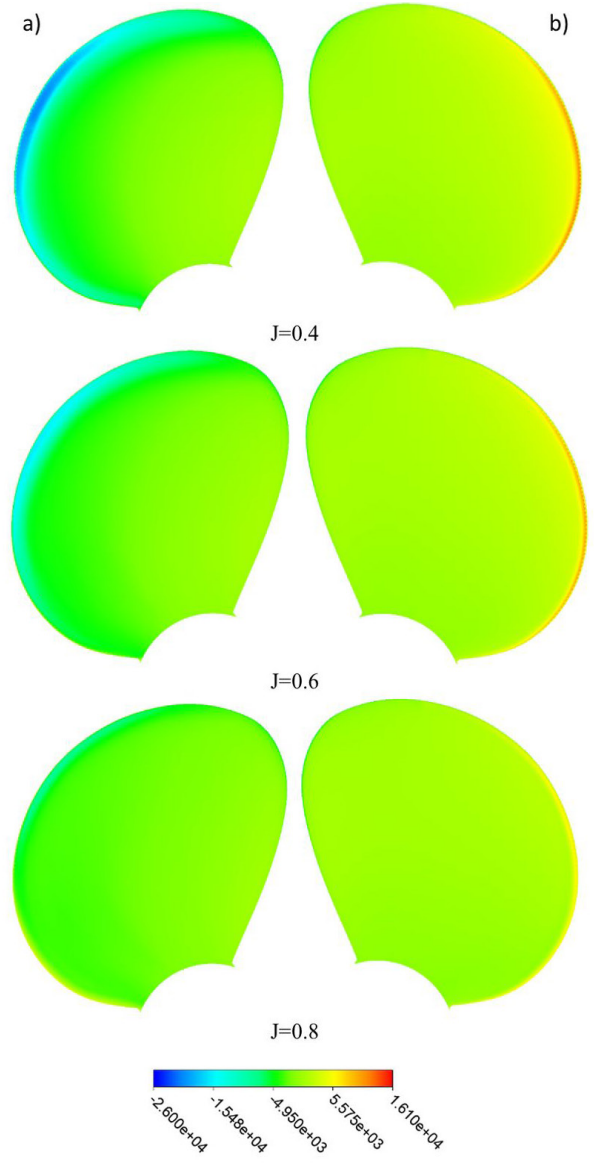

Figure 5. *Pressure distribution on a) pressure surface and b) suction surface*

3. Results and Discussion

The B-5 propeller was subjected to CFDs simulations. A sequence of modifications, ranging from J=0 to J=1, yielded pressure distribution data on the propeller, with particular attention paid to the blade, which will require additional analysis to determine the impact of the pressure on the material on the blade.

The results of the open-water simulation with the CFD method obtained results in the form of pressure distribution, which will then be used as input from structural analysis. Figure 6 shows the pressure distribution that was produced by the CFD simulation. with a pressure surface and a suction. Furthermore, data analysis was carried out by comparing the simulation results on open water with the CFDs method with data on the Wageningen B-Series Propellers curve. The results are obtained in Figure 7. Experimental data were obtained using calculations to validate numerical results. Non-dimensional thrust and torque coefficients, efficiency values, and cavity patterns on the blades are examples of such parameters.

Table 2. *Carbon fiber Ply angle*

Unidirectional tape prepreg	Woven fabric prepreg
0 Ply	0 Ply
+45 Ply	90 Ply
-45 Ply	+45 Ply
90 Ply	-45 Ply

Testing by comparing several lightweight materials like carbon fiber has been carried out. This is useful for choosing the lightest carbon fiber material and will be used as a sample in this study. There are metallic and non-metallic materials such as bronze, titanium alloy, copper alloy, epoxy carbon fiber UD, and epoxy carbon fiber Woven and carbon fiber.

Therefore, in this analysis, two of the lightest carbon fiber materials were taken, namely, epoxy carbon fiber UD and epoxy carbon fiber Woven, with masses of 8.65 E-02 kg

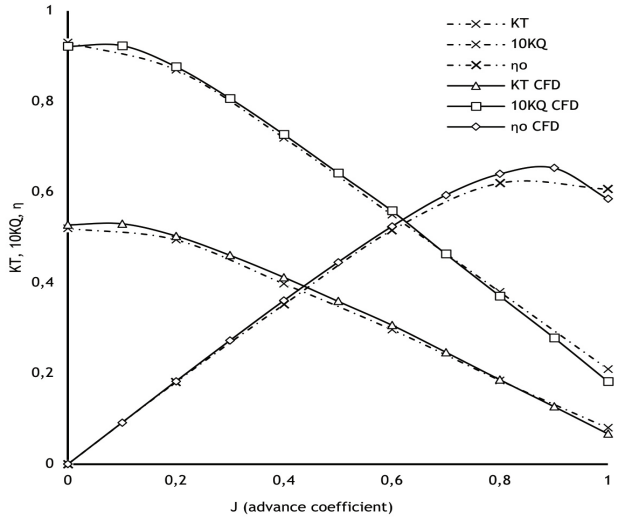

Figure 6. *Open-water test comparisons between the numerical and experimental results for propeller propulsion performance*

Table 3. *Properties of material assignment (ANSYS engineering data)*

Properties of the materials	Composite, epoxy/CF, UD prepreg, QI		Composite, epoxy/CF, woven prepreg, QI	
Density	1565	kg/mm³	1575	kg/mm³
Young's modulus	5.465e+10	Pa	4.616e+10	Pa
Poisson's ratio	0.306		0.337	
Bulk modulus	4.695e+10	Pa	4.7198e+10	Pa
Shear modulus	2.0923e+10	Pa	1.7263e+10	Pa
Isotropic secant coefficient of thermal expansion	1.203e-06	1/°C	1.27e-05	1/°C
Tensile ultimate strength	6.667e+08	Pa	5.402e+08	Pa
Tensile yield strength	6.667e+08	Pa	5.402e+08	Pa
Properties of the materials	**Titanium alloy**		**Copper alloy**	
Density	4620	kg/mm³	8300	kg/mm³
Young's modulus	9.6e+10	Pa	1.1e+11	Pa
Poisson's ratio	0.36		0.34	
Bulk modulus	1.1429e+11	Pa	1.1458e+11	Pa
Shear modulus	3.5294e+10	Pa	4.1045e+10	Pa
Isotropic secant coefficient of thermal expansion	9.4e-06	1/°C	1.8e-05	1/°C
Tensile ultimate strength	1.07e+09	Pa	4.3e+08	Pa
Tensile yield strength	9.3e+08	Pa	2.8e+08	Pa

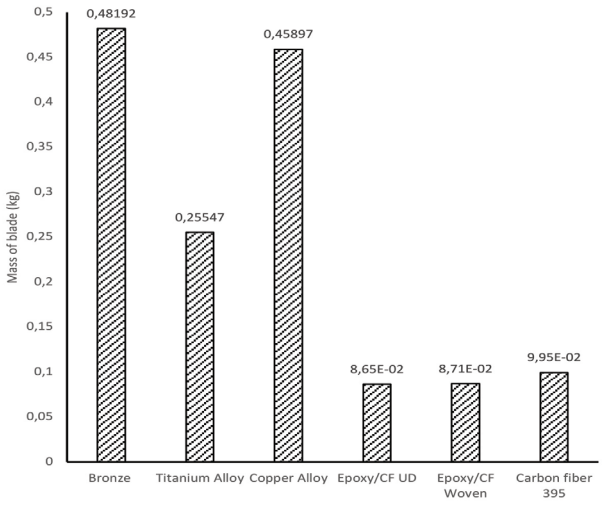

Figure 7. *Material weight comparison of propeller blades*

and 8.71 E-02 kg, respectively. When compared to metallic materials such as copper alloys with non-metallic materials such as epoxy carbon fiber UD, a ratio value of 1:5 was obtained.

Two varieties of carbon fiber were used in this investigation for each parameter by the result of. Using materials that have been dispersed in CFD simulations as pressure loads on open-water tests at values J=0 to J=1, the first parameter simulates testing with loads in the form of pressure. Epoxy carbon fiber UD and epoxy carbon fiber Woven are the materials. In addition, the outcomes of both material types will be shown in J values in accordance with the ship's operating conditions.

3.1. Blade Deformation

The results of these two materials are compared with the deformation of two metallic materials, titanium alloy and copper alloy, as a reference for comparison of the total deformation values. In Figure 8, compared to four materials

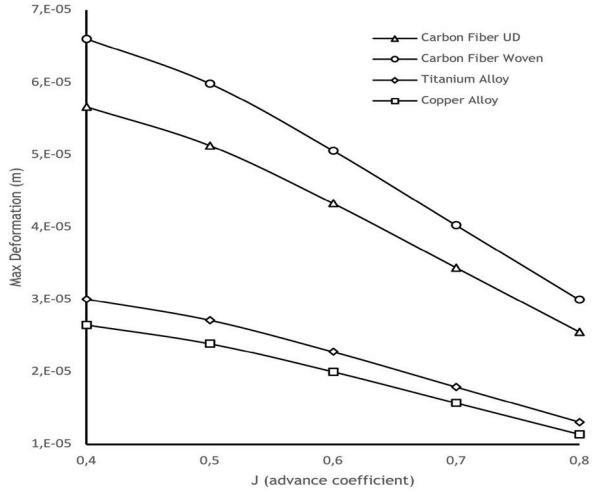

Figure 8. *Maximum deformation curve*

in the curve in the range of J=0.4-0.8. From metallic materials, the deformation value of copper alloy is smaller than that of titanium alloy, while in non-metallic materials, the deformation value of the epoxy carbon fiber UD material is lower than that of the epoxy carbon fiber Woven. In general, both non-metallic materials have a relatively similar deformation trend when compared to metallic materials; in other words, these non-metallic materials have a reasonable deformation value because of their properties.

Deformation on the blade is then analyzed on the basis of the blade section, with a range of numbers 1-15 corresponding to Figure 9. Starting from blade section 1 is the largest deformation value, then continuing down until blade section 15 is the smallest value. On the curve, the deformation value is displayed on the basis of the blade section for four comparison materials. The curve in metallic materials tends to slope compared with non-metallic materials or carbon fibers, which have a significant difference in deformation values in each blade section. Of course, this is a consideration in analyzing propellers with carbon fiber material using metallic material references. This is only limited to analyzing and detailing the results of blade deformation in the adjusted section, and the deformation results will be displayed in the form of contour only.

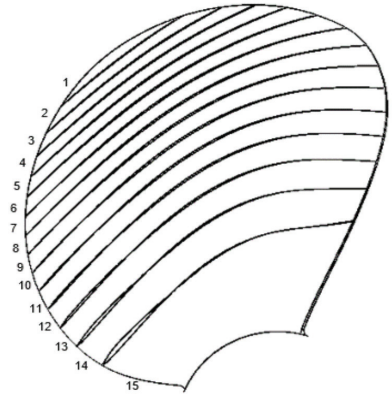

Figure 9. *Blade section of the propeller*

Furthermore, the results of this deformation are depicted on Figure 10-14 illustrates how variations in the form of carbon fibers impact the strength of the blades under load, causing these two materials maximum total deformation at the blade tips to differ. From the results of structural analysis with a fluid structure interaction approach, the largest deformation value was obtained in epoxy carbon fiber woven material at a value of J=0.4 of 6.81E-05m. and the lowest deformation value was in copper alloy material at J=0.8 of 1.34E-05m. When compared to non-metallic materials, the deformation value of epoxy carbon fiber UD is quite low, with a difference of 4.44E-06m, compared to epoxy carbon fiber woven at J=0.8.

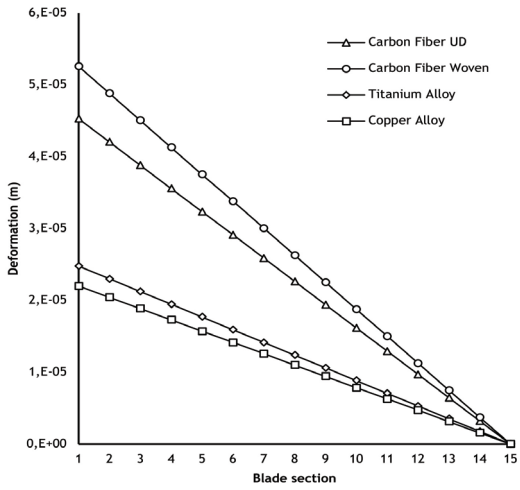

Figure 10. *Maximum deformation by blade section at J=0.6*

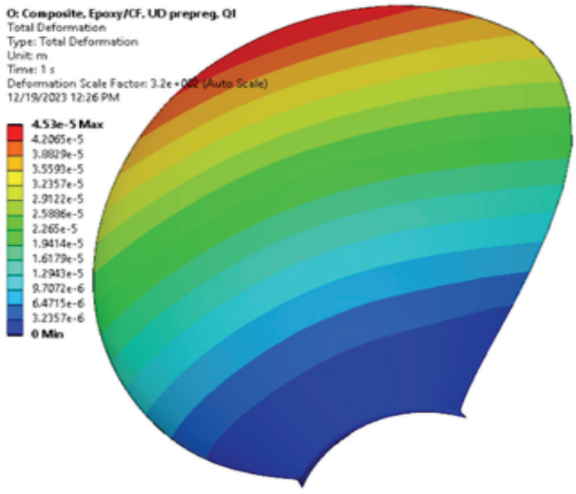

Figure 11. *Maximum deformation c/f UD at J=0.6*

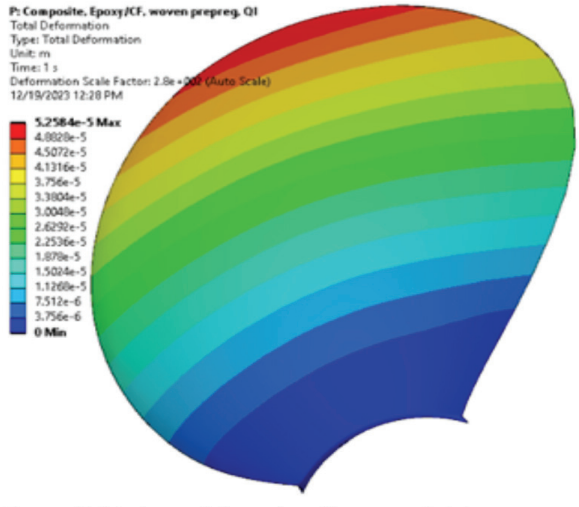

Figure 12. *Maximum deformation c/f woven at J=0.6*

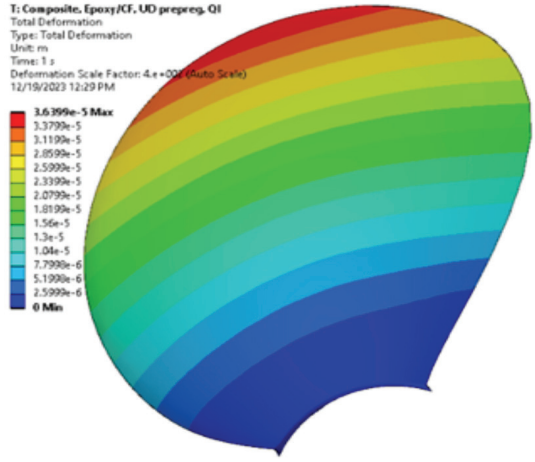

Figure 13. *Maximum deformation c/f UD J=0.7*

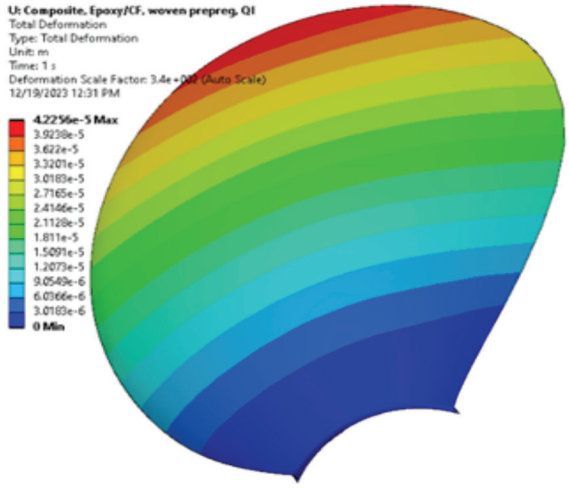

Figure 14. *Maximum deformation c/f woven at J=0.8*

It is clear from the data in the table and curve that woven and carbon fiber UD deformation is significantly greater than that of metallic materials like copper and titanium alloys.

Maximum blade deformation occurs in a carbon fiber woven material, with an illustration of comparison with solid materials that do not deform according to the illustration in Figure 15.

Blade stress analysis was carried out by inputting data from the results of the open water test in the form of pressure at conditions J=0.4 to J=0.8. Figure 16 illustrates how the data comparison is produced as a curve. The curve above show that UD carbon fiber has a low value, ranging from J=0.4 to J=0.8. This suggests that these two materials respond differently to loads.The results of equivalent (von-misses) stress tend to be identical in results. each J value. For carbon

fiber materials, there is a maximum equivalent (von-misses) stress that is different from the two materials above. The difference occurs with a fairly large difference in value between 4.43E+06 Pa and 4.51E+06 Pa, the minimum value between 37170 Pa and 41713 Pa. This greater value for the carbon fiber woven material indicates that the response to the load received by this material has a greater value. Here, there is a difference between the maximum value and the minimum value.

Additionally, the maximum equivalent (von-misses) stress values for metallic materials values of maximum equivalent (von-misses) stress are 4.60E+06 Pa and 4.52E+06 Pa respectively and minimum values are 32870 Pa for Titanium Alloy and 33482 Pa for Copper Alloy. Compared with previous results at J=0.6, the minimum stress distribution value has a relatively small difference. At both the pressure surface and suction surface positions, which are dominated by the minimal stress value throughout nearly the entire blade surface, the stress distribution patterns in the image are identical to one another. Figure 17 to Figure 20 illustrates the difference in maximum equivalent (von-misses) stress

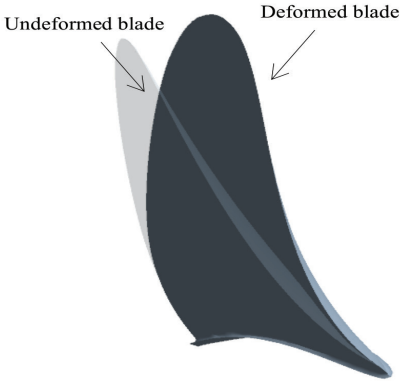

Figure 15. *Undeformed and deformed blade carbon fiber woven material under maximum load*

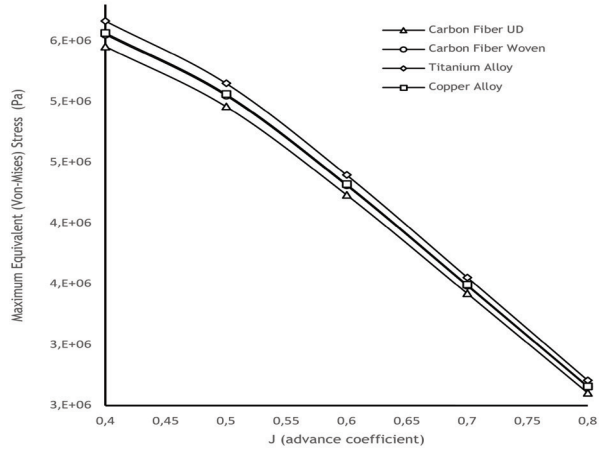

Figure 16*. Maximum equivalent (von-misses) stress curve*

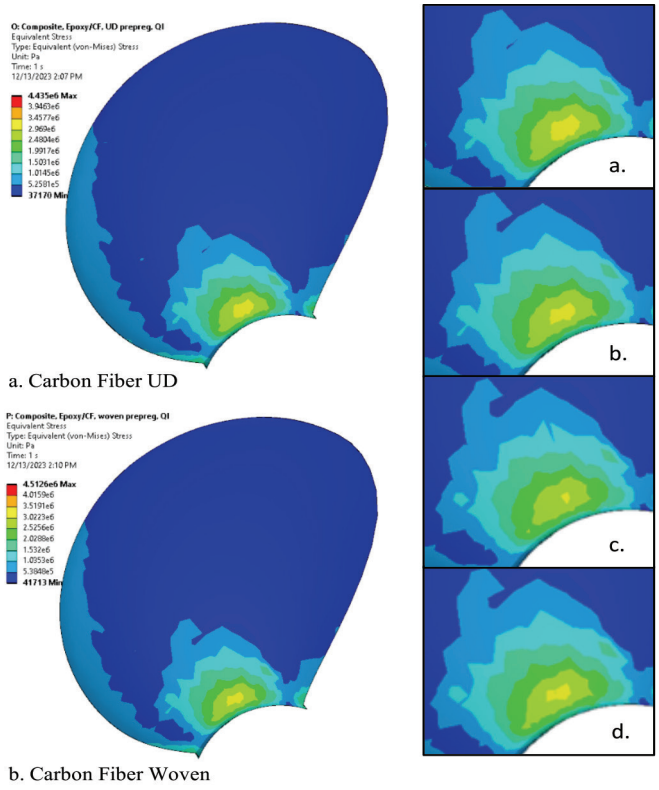

Figure 17. *Equivalent (von-misses) stress at J=0.6 carbon fiber materials, suction surface*

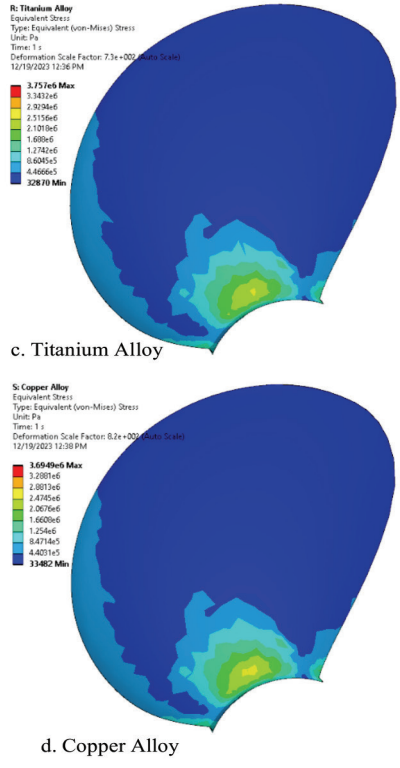

Figure 18. *Equivalent (von-misses) stress at J=0.6 metallic materials suction surface*

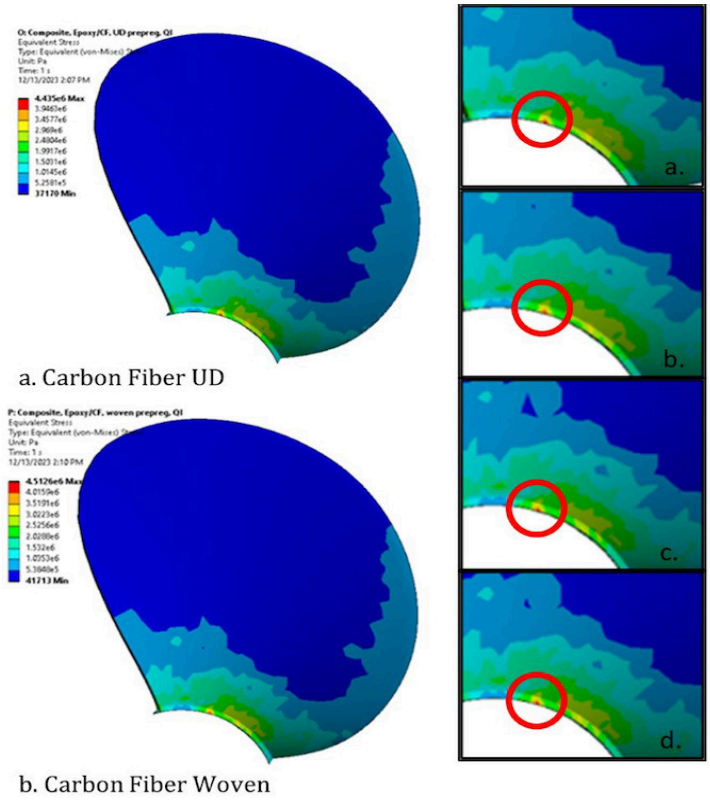

Figure 19. *Equivalent (von-misses) stress at J=0.6 carbon fiber materials, pressure surface*

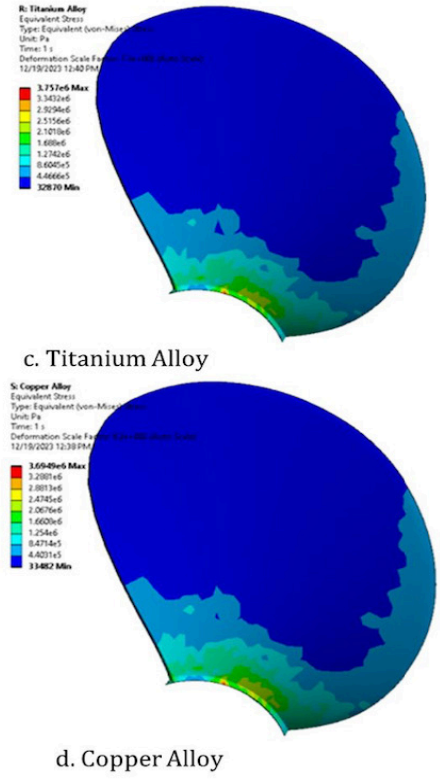

Figure 20. *Equivalent (von-misses) stress at J=0.6 metallic materials, pressure surface*

in carbon fiber UD and carbon fiber woven materials by comparing them with metallic materials such as titanium alloy and copper alloy. The stress distribution on the UD carbon fiber material is often smaller than that on the woven carbon fiber material.

The equivalent (von-misses) stress results at J=0.6 for both materials tend to follow the same pattern at the propeller's pressure and suction surface locations, with the minimal stress distribution coefficient being the determining factor. Looking at Table 2, it is clear that the maximum equivalent (von-misses) stress can still be tolerated; therefore, even if it is at the bottom of the limit, it is not an issue.

4. Conclusion

In this study, a series of simulations on the use of carbon fiber in a B-5 propeller were carried out. The research has been completed with the following conclusions. From the results of the comparison of metallic and non-metallic materials, it can be concluded that the mass of the blade for epoxy carbon fiber material, both UD and woven, is five times lighter than that of copper alloy material, which has the advantage of the mass of the blade material being much lighter.

Thus, the use of this material can certainly be an alternative choice of material in marine propellers. It can be concluded that the epoxy carbon UD material is better and has a low deformation and equivalent (Von-Mises) stress value when compared to epoxy carbon fiber woven material. It is highly recommended to use the epoxy carbon UD prepreg material for marine propeller use. Deformation of the blade is caused by the pressure received by the propeller blade, so the influence of pressure affects the value of deformation in the blade. This can be used as a further analysis of the optimum design laminate of carbon fiber on the blade propeller.

Of course, this research can still be developed further by examining how deformation or deflection affects the propeller's operational efficiency, whether the effects of deformation interfere with performance or can increase the energy efficiency of the propeller, or in other words, improve the performance of the propeller compared to general propeller materials. Additionally, deformation of the propeller blades will result in deflections, which will undoubtedly impair the marine propeller's operational performance in future analysis.

In addition, the deformation of the propeller will result in deflection, which will undoubtedly affect the operational performance of the marine propeller, whether to further increase or decrease the propeller's performance in future analysis.

Acknowledgment

We express our sincere gratitude to the Marine Power and Propulsion Laboratories, Department of Marine Engineering, Institut Teknologi Sepuluh Nopember.

Authorship Contributions

Concept design: F. I. Ahsan, I. M. Ariana, and A. Z. M. Fathallah, Data Collection or Processing: F. I. Ahsan, Analysis or Interpretation: F. I. Ahsan, I. M. Ariana, and A. Z. M. Fathallah, Literature Review: F. I. Ahsan, I. M. Ariana, and A. Z. M. Fathallah, Writing, Reviewing and Editing: F. I. Ahsan, I. M. Ariana, and A. Z. M. Fathallah.

Funding: The authors declare that no funds, grants, or other support was received during the preparation of this manuscript.

References

[1] Derek Hull. Engineering with fibre-polymer laminates: By peter powell. chapman & hall, london, 1994 (441 pp.+ xvii). isbn 0 412 496100 (hb). Greene, E. (1997). Design Guide for Marine Applications of Composites, SSC-403, Jan 1997.

[2] Y. L. Young, J. W. Baker, and M. R. Motley, "Reliability-based design and optimization of adaptive marine structures". *Composite Structures,* vol 92, pp. 244-253, Jan 2010.

[3] B.-G. Paik, et al. "Investigation on the performance characteristics of the flexible propellers". *Ocean Engineering,* vol. 73, pp. 139-148, Nov 2013.

[4] Y. L. Young, M. R Motley, R. Barber, E. J. Chae, and N. Garg, "Adaptive composite marine propulsors and turbines: progress and challenges". *Applied Mechanics Reviews,* vol. 68, 060803, Nov 2016.

[5] I. M. Ariana, R. B. Prihandanu, D. W. Handani, and A. A. B. Dinariyana, "Investigation of the effects of the pre-duct in a ship on propeller–hull interactions using the CFD method". *CFD Letters,* vol. 15, pp. 17-30, 2023.

[6] I. Fikry, I. M. Ariana, and C. Kusuma, "Propeller performance analysis on the modification of trailing edge shape as anti-singing". *IOP Conference Series: Earth and Environmental Science*, vol. 1166, 012005, 2023.

[7] A. Purwana, I. M. Ariana, and W. Wardhana, "Numerical study on the cavitation noise of marine skew propellers". *Journal of Naval Architecture and Marine Engineering,* vol. 18, pp. 97-107, Dec 2021.

[8] J. W. Cohen. *On stress calculations in helicoidal shells and propeller blades*. Waltman, 1955.

[9] P. Atkinson, "On the choice of method for the calculation of stress in marine propellers". *Trans RINA,* vol. 110, pp. 447-463, 1968.

[10] S. Paboeuf, B. Collier, P. Berthelot, F. Le Lay, and L.-A. Vialle, "Composite blade propeller: a design assessment approach". *chez 4th International Conference on Mechanics of Composites*, 2018.

[11] F. Zhang, and J. Ma, "FSI analysis the dynamic performance of composite propeller". Conference: ASME 2018 37th International Conference on Ocean, Offshore and Arctic Engineering, Jun 2018.

[12] R. Vijayanandh, K. Venkatesan, M. Senthil Kumar, G. Raj Kumar, P. Jagadeeshwaran, and R. Raj Kumar,"Comparative fatigue life estimations of marine propeller by using FSI". *Journal of Physics: Conference Series,* vol. 1473, 012018, 2020.

[13] G. Yang, X. Ying, and H. Zheng, "Computation of composite propeller's two-way fluid-structure coupling". *Ship Science and Technology,* vol. 37, pp. 16-20, 2015.

[14] Z. Huang, Y. Xiong, and H. T. Sun, "Thicken and pre-deformed design of composite marine propellers". *Journal of Propulsion Technology,* vol. 38, pp. 2107-2114, 2017.

[15] Z. Huang, Y. Xiong, and G. Yang, "A fluid-structure coupling method for composite propellers based on ANSYS ACP module". *Jisuan Lixue Xuebao/Chinese Journal of Computational Mechanics,* vol. 34, pp. 501-506, Aug 2017.

[16] Z. Huang, Y. Xiong, and G. Yang, "A comparative study of one-way and two-way fluid-structure coupling of copper and carbon fiber propeller". *J Nav Univ Eng,* vol. 29, pp. 31-35, 2017.

[17] S. Han, H. Lee, M.C. Song, Chang, B. J. Investigation of hydro -elastic performance of marine propellers using fluid-structure interaction analysis, ASME Int. Mech. Eng. Congr. Expo. Proc. 7A –2015.

[18] H. Lee, M. C. Song, S. Han, B. Chang, and J.-C. Suh, "Hydro-elastic aspects of a composite marine propeller in accordance with ply lamination methods". *Journal of Marine Science and Technology,* vol. 22, pp. 479-493, Jan 2017.

[19] J. Carlton, *Marine propellers and propulsion*. Elsevier Science, 4th edition, 2012.

[20] Ö. K. Kınacı, and C. Delen, "Advancing computational hydroacoustics for marine propellers: investigating the limits of incompressible solvers in far-field noise prediction". *Journal of ETA Maritime Science*, vol. 11, pp. 110-118, Jun 2023.

[21] Ş. Bal, "Numerical investigation of propeller skew effect on cavitation". *Journal of ETA Maritime Science*, vol. 7, pp. 127-136, Jun 2019.

[22] K. Yu, P. Yan, and J. Hu, "Numerical analysis of blade stress of marine propellers". *Journal of Marine Science and Application,* vol. 19, pp. 436-443, Oct 2020.

[23] M. R. Motley, Z. Liu, and Y. L. Young, "Utilizing fluid–structure interactions to improve energy efficiency of composite marine propellers in spatially varying wake". *Composite Structures,* vol. 90, pp. 304-313, Oct 2009.